Social Cognitive and Affective Neuroscience Advance Access published October 29, 2015

Social Cognitive and Affective Neuroscience, 2015, 1–10

doi: 10.1093/scan/nsv123
Original article

Parallel processing of general and specific threat during early stages of perception

Yuqi You and Wen Li

Department of Psychology, Florida State University, Tallahassee, FL 32306, USA

Correspondence should be addressed to: Yuqi You and Wen Li, Department of Psychology, Florida State University, 1107 W. Call St, Tallahassee, FL 32306, USA. Email: you@psy.fsu.edu or wenli@psy.fsu.edu

Abstract

Differential processing of threat can consummate as early as 100 ms post-stimulus. Moreover, early perception not only differentiates threat from non-threat stimuli but also distinguishes among discrete threat subtypes (e.g. fear, disgust and anger). Combining spatial-frequency-filtered images of fear, disgust and neutral scenes with high-density event-related potentials and intracranial source estimation, we investigated the neural underpinnings of general and specific threat processing in early stages of perception. Conveyed in low spatial frequencies, fear and disgust images evoked convergent visual responses with similarly enhanced N1 potentials and dorsal visual (middle temporal gyrus) cortical activity (relative to neutral cues; peaking at 156 ms). Nevertheless, conveyed in high spatial frequencies, fear and disgust elicited divergent visual responses, with fear enhancing and disgust suppressing P1 potentials and ventral visual (occipital fusiform) cortical activity (peaking at 121 ms). Therefore, general and specific threat processing operates in parallel in early perception, with the ventral visual pathway engaged in specific processing of discrete threats and the dorsal visual pathway in general threat processing. Furthermore, selectively tuned to distinctive spatial-frequency channels and visual pathways, these parallel processes underpin dimensional and categorical threat characterization, promoting efficient threat response. These findings thus lend support to hybrid models of emotion.

Key words: threat encoding, sensory, visual cortex, amygdala, spatial frequency

Introduction

Efficient detection of signals of danger in the environment is a hallmark of adapative behavior. Extensive electrophysiological data (recorded on the scalp or directly on the visual cortex) have revealed remarkable efficiency in visual categorization of threat-laden faces or scenes, consummating at about 100 ms post-stimulus or even earlier (cf. Vuilleumier and Pourtois, 2007; Olofsson *et al.*, 2008; Miskovic and Keil, 2012). Notably, this feat is achieved not only for evolutionarily privileged stimuli (e.g. faces; Pizzagalli *et al.*, 2003; Eimer and Holmes, 2007; Forscher and Li, 2012; Kawasaki *et al.*, 2012; Flaisch and Schupp, 2013) or simple cues (e.g. geometric shapes; Stolarova *et al.*, 2006; Steinberg *et al.*, 2013;), but also for complex scenes (Keil *et al.*, 2002; Smith *et al.*, 2003; Carretié *et al.*, 2004, 2007; Hot *et al.*, 2006; Alorda *et al.*, 2007; Krusemark and Li, 2011, 2013). Moreover, this fast processing of threat can be exaggerated in anxious individuals characterized by heightened sensitivity and reactivity to threat stimuli, pointing to an early perceptual mechanism underlying the pathophysiology of anxiety disorders (Williams *et al.*, 2007; Li *et al.*, 2008b; Weinberg and Hajcak, 2011; Rossignol *et al.*, 2012).

Recent studies further suggest that this early threat processing not only differentiates threat from non-threat (neutral or positive) stimuli (along general dimensions of affective valence/arousal; Russell, 1980), but is also capable of dissociating individual basic emotions (Ekman, 1992), even within the domain of threat (e.g. fear, disgust and anger). Replicated findings indicate divergent processing of fear and disgust during early perception: relative to neutral scenes, fear-evoking scenes enhance whereas disgust-evoking scenes suppress visual event-related potentials (ERPs; e.g. the P1 component, an early visual ERP peaking around 100 ms) and concomitant extrastriate cortical activity (Krusemark and Li, 2011, 2013). Importantly, these opposite deviations for fear and disgust processing (from the

Received: 6 May 2015; **Revised:** 10 September 2015; **Accepted:** 21 September 2015

neutral condition) highlight qualitative differentiation of discrete threat subtypes beyond their quantitative (dimensional) differences in arousal, intensity or valence. In keeping with that, another group demonstrates an augmented P1 component to angry faces and a suppressed P1 to disgusted faces, relative to neutral faces (Liu *et al.*, 2015), providing further support for early visual discrimination of threat subtypes.

This specialized threat processing aligns with categorical/basic theories of emotion, permiting-specific characterization of discrete emotions serving specific biological functions (Ekman, 1992; Izard, 1994). To the extent that they are both threat relevant, fear and disgust are posited to subserve independent biological systems—the ‘self protection system’ and the ‘disease avoidance system’, respectively (Rozin and Fallon, 1987; Oaten *et al.*, 2009; Neuberg *et al.*, 2011), and accordingly, each represents core emotions in specific subtypes of anxiety (e.g. fear for social anxiety; disgust for blood phobia; McNally, 2002). In sensory processing, fear purportedly elicits an immediate ‘stop-look-and-listen’ response to facilitate sensory acquisition in order to guide action (e.g. fight or flight; Gray, 1987), while disgust provokes instant sensory rejection to prevent poison or contamination from entering the organism (Rozin and Fallon, 1987). Interestingly, these opposing sensory responses align with the contrary biomechanical properties in facial expressions of fear and disgust: the widened eyes and nostrils in fearful faces augment visual and oflactory sensory intake, contrasting with narrowed eyes and nostrils in disgusted faces that restrict sensory intake (Susskind *et al.*, 2008). Therefore, it would make important ecological sense that fear and disgust stimuli engage specific processing during early perception, thereby promoting corresponding responses with minimal delay.

Nevertheless, a key question remains as to how the sensory system manages to differentially encode threat subtypes at such a fast speed. It is commonly thought that a ‘quick-and-dirty’ subcortical (superior-colliculus-pulvinar) pathway transmits coarse features of threat stimuli to the amygdala, where threat information is extracted and fedback to the visual cortex to support threat perception (Phelps and LeDoux, 2005; Vuilleumier and Pourtois, 2007). The orbitofrontal cortex (OFC) may also extract threat value based on crudely processed visual input and in turn inform threat perception via reentrant feedback to the visual cortex (Barrett and Bar, 2009; Kveraga *et al.*, 2007). However, to the extent that convincing evidence exists for threat processing in the amygdala and OFC, these findings typically indicate generalized/dimensional response enhancement to biologically salient stimuli (e.g. fear, disgust, or reward) relative to neutral stimuli (Phillips *et al.*, 1998; Anderson *et al.*, 2003; Rolls, 2004), providing little insights into specialized characterization of threat subtypes in the brain (Lindquist *et al.*, 2012).

Altenatively, although simple sensory inputs (e.g. a tone or a light; as often used in classical conditioning) can be transmitted to the amygdala via the subcortical pathway, complex stimuli (e.g. scenes) would require elaborate processing in the sensory cortex before eliciting emotion processing in the limbic system (Phelps and LeDoux, 2005). Indeed, meta-analyses of neuroimaging data indicate that besides the amygdala and OFC, emotional scenes reliably activate the occipital visual areas (e.g. the lateral occipital cortex), which are critical for visual object processing (Sabatinelli *et al.*, 2011; Lindquist *et al.*, 2012). Moreover, recent computational modeling of fMRI data suggests that sensory cortical feedforward input is essential for threat processing in the amygdala (Kumar *et al.*, 2012; Krusemark *et al.*, 2013). Therefore, early encoding of fear and disgust may recruit multiple neural pathways in parallel (Pessoa and Adolphs, 2010; Chikazoe *et al.*, 2014), entailing coarse coding of valence and/or arousal in the limbic/paralimbic areas and fine-grained categorization of discrete threat emotions in the sensory cortex.

To further validate specific threat processing in early visual perception and more importantly, to elucidate its neural unpderpinnings, we combined spatial-frequency-filtered images of natural scenes of fear or disgust (Figure 1) with high-density electroencephalogram (EEG) recordings and cortical source estimation (focusing particularly on early visual ERPs). Compelling evidence indicates that high spatial frequencies (HSFs) largely contribute to refined perception subserved by the ventral visual cortex while low spatial frequencies (LSFs) largely contribute to coarse perception subserved by subcortical and dorsal visual cortical pathways (Shulman and Wilson, 1987; Livingstone and Hubel, 1988; Hughes *et al.*, 1990; Merigan and Maunsell, 1993; Schyns and Oliva, 1994; Robertson, 1996; Han *et al.*, 2003; Vuilleumier *et al.*, 2003; Loftus and Harley, 2005; Yoshida and Yoshino, 2007; Flevaris *et al.*, 2010; De Cesarei *et al*, 2013; Kauffmann *et al.*, 2015). We therefore filtered images to include either HSFs or LSFs to isolate different early visual processes. We hypothesized that distinct visual processing of fear and disgust would emerge in the HSF images and be source-localized to the ventral visual cortex, reflecting cortical-based, refined encoding of discrete threats, whereas overlapping visual processing of fear and disgust would arise in the LSF images and be localized to the dorsal visual cortex, reflecting general, dimensional processing of threat that is likely to be intimately associated with limbic emotion processing.

Materials and methods

Participants

Forty-six right-handed college students (mean age, 19.3 years; 22 men) with normal or corrected-to-normal vision participated in the study. Six participants were excluded from EEG analysis due to excessive eye movements, trial omissions and recording failures. All participants denied a history of severe head injury, psychological/neurological disorders or current use of psychotropic medication. All participants provided informed consent to participate in this study, which was approved by the University of Wisconsin Institutional Review Board.

Stimuli

Twenty-seven broadband images were selected from the International Affective Picture Set (Lang *et al.*, 2008) and internet sources, depicting natural scenes/objects (nine for each emotion category). The fear set included objects of snakes, spiders, guns and knives; the disgust set included roaches, dirty toilets and vomit, and the neutral emotion set included household objects (Fig. 1A). To generate LSF and HSF images, the unfiltered, broadband images were transformed to grayscale and equal size, normalized to equal luminance (17.11 cd/m^2), and low-pass filtered at three cycles/degree or high-pass filtered at seven cycles/degree, respectively (Figure 1A; Vuilleumier *et al.*, 2003; Winston *et al.*, 2003; Vlamings *et al.* 2009). We note that our previous studies (Krusemark and Li, 2011, 2013) have examined these emotions in broadband, unfiltered images. Therefore, to prevent fatigue and limit image repetition, we examined expressly responses to the filtered images here. Systematic imaging processing using SHINE (Willenbockel *et al.*, 2010) and in-house

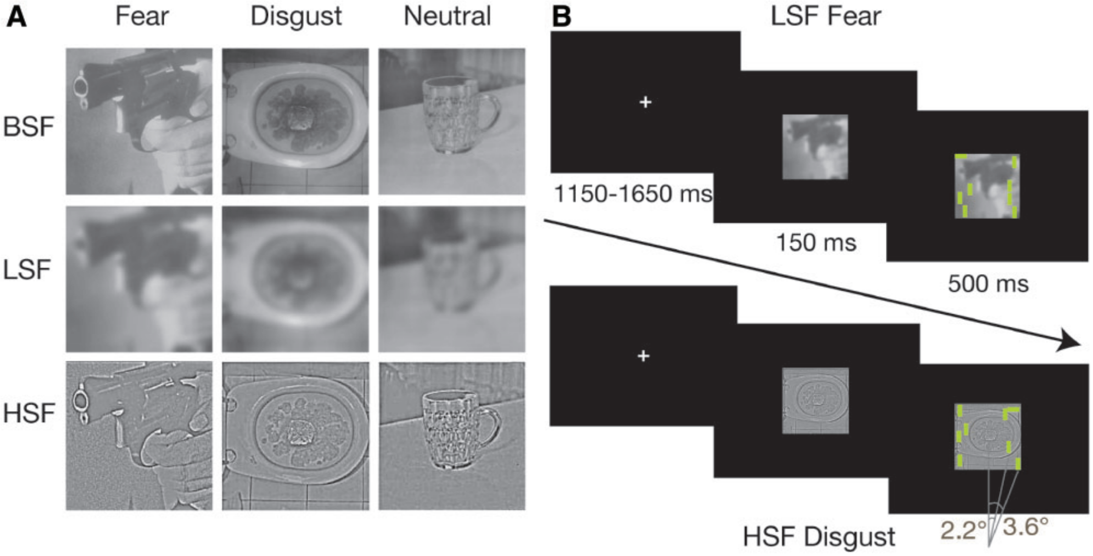

Fig. 1. Example stimuli and experimental paradigm. Twenty-seven gray-scale broadband images (nine for each emotion category) were filtered to contain either LSF or HSF information, forming a 3 × 2 factorial design of emotion and SF. Luminance, contrast and wavelet power were equated across image sets. **(A)** Example stimuli for each emotion category in broadband, LSF and HSF versions are displayed. **(B)** Participants performed a visual search task: Following an emotion image (150 ms), a search array was superimposed on the image (500 ms), and participants responded as to which quadrant contained the target (horizontal bar) by button-pressing.

programs was performed to ensure the resultant six image sets (H/LSF × Fear/Disgust/Neutral) were equated on luminance [124 (0.01) on a 0–255 scale] and contrast [32 (0.08)]. Wavelet analyses (Delplanque *et al.*, 2007) were applied to filtered image sets to ensure equal wavelet energy for each spatial frequency (SF) band across three emotion conditions (P's > 0.289). Lastly, objective measures of visual complexity (edge density, entropy, compressed image size; Rosenholtz *et al.*, 2007; Marin and Leder, 2013) were computed and submitted to ANOVAs (Emotion-by-SF), which revealed no significant effect of emotion or emotion-SF interaction on visual complexity (P's > 0.397; see Supplementary Materials for details).

Furthermore, an independent group ($N = 14$) provided ratings of emotional content (valence, arousal, disgust and fear) and image recognizability on a visual analogue scale, while another group ($N = 11$) provided familiarity ratings on these images. Results verified the emotional content of image sets and indicated comparable content recognizability and familiarity (P's > 0.463) across emotion conditions (see Supplementary Materials for details).

Main experiment

Participants were seated ~120 cm from a cathode ray tube (CRT) monitor in an electrically shielded room, and performed a visual search task adapted from a previous study (Krusemark and Li, 2011; Figure 1B). There were six conditions [Emotion (fear, disgust, neutral) × Spatial Frequency (LSF, HSF)], each including 100 trials randomly presented in four experimental blocks. Each trial began with a crosshair at the center of the screen, followed by an image ($7.2^\circ \times 7.2^\circ$) centrally displayed for 150 ms. Next, a search array in green was superimposed on the image for 500 ms, consisting of one horizontal bar (target) and seven vertical bars (distracters). Participants were required to make a button press to indicate the quadrant where the target was located while maintaining fixation.

Stimulus presentation was linked to the refresh rate (60 Hz) of the CRT monitor and delivered using Cogent2000 software (Wellcome Department, London, UK) as implemented in Matlab (Mathworks, Natick, MA). EEG was recorded throughout the experiment. Synchronization between stimulus display and data acquisition was verified using a photodiode placed at the center of the monitor screen.

Control EEG experiment

To further rule out artifact induced by potential physical disparities across the image sets, we then conducted a control EEG experiment in the same participants. The same visual search task and EEG acquisition and analysis parameters used in the main experiment were adopted here except that the images were phase-scrambled (Chen *et al.*, 2007) and thus unintelligible.

EEG recording and analysis

EEG were recorded from a 96-channel (BioSemi ActiveTwo) system at a 1024 Hz sampling rate, down-sampled to 256 Hz, and digital bandpass filtered from 0.1 to 40 Hz. Electrooculogram (EOG) was recorded at two eye electrodes at the outer canthi of each eye and one infraorbital to the left eye. The epoch was segmented from −200 to 300 ms post stimulus onset to focus on early visual processing, corrected to the 200-ms pre-stimulus baseline. Trials with EEG/EOG voltages exceeding $\pm 75\,\mu V$ (relative to pre-stimulus baseline) were excluded from analysis.

We focused on a well-established visual ERP component, the P1 potential (peaking at ~100 ms), reflecting early visual processing in the extrastriate cortex (Mangun *et al.*, 1993). Inspection of grand average waveforms indicated a P1 component that peaked at 121 ms post-stimulus, maximal at central occipital sites. We also examined the N1 potential, another key visual ERP peaking around 150–190 ms (Hillyard and Anllo-Vento, 1998; Vogel and Luck, 2000). Grand average waveforms indicated a distinct N1 component that peaked at 156 ms post-stimulus, also maximal at occipital sites. Given this occipital distribution, the absence of a laterality hypothesis, and a lack of relevant site effects, we decided to focus on the more commonly used Oz site in our analysis. Mean P1 and N1 amplitudes were extracted at Oz over 36 ms (105–141 ms) and 44 ms (137–181 ms) intervals centered on the corresponding peaks (i.e. peak ± 4 and 5 data points, respectively, determined based on the widths of these components).

Lastly, to depict the evolving time course more closely and to identify the latencies of threat processing, we then performed a data-driven analysis (Krusemark and Li, 2013). We submitted voltage amplitude at each data point to paired *t*-tests (fear *vs* disgust, fear *vs* neutral and neutral *vs* disgust in HSF and LSF). To control for Type I error, a corrected $P < 0.05$ was set based on Monte Carlo simulation, represented by a significance threshold of $P < 0.05$ over 11 consecutive data points. The first time point of the significance window was identified as the latency of discrimination (see Supplementary Materials for details).

Low-resolution brain electromagnetic tomography. We then isolated the cortical sources of significant ERP effects using low-resolution brain electromagnetic tomography (LORETA). As an inverse solution, LORETA has been validated using neuroimaging methods in visual and cognitive processes (Pascual-Marqui *et al.*, 2002). To minimize false positives in intracranial source localization, we applied constraints in our analyses to the time windows and tests where surface ERP effects were significant (Thatcher *et al.*, 2005; Krusemark and Li, 2013). Also, based on Monte Carlo simulation, we derived a corrected threshold of $P < 0.05$, requiring a voxel-level $P < 0.005$ over three contiguous voxels. All coordinates are reported in MNI space. Specific details are provided in Supplementary Materials.

Statistical analysis

Two-way repeated measures analyses of variance (ANOVAs; with Greenhouse-Geisser corrections) with independent variables of Emotion (fear, disgust, neutral) and SF (LSF, HSF) were performed on response time (RT), accuracy and P1/N1 mean amplitudes. Significant ANOVA effects were followed by *t*-tests to contrast the effects of individual conditions (using the least significant difference test; LSD). RTs over ± 2 SDs from each subject's mean RT were excluded from analysis.

Results

General threat-related interference in visual search

A repeated-measures ANOVA of Emotion and SF revealed a SF effect [$F(1,45) = 54.54$, $P < 0.001$, $\eta_p^2 = 0.55$] and an emotion effect [$F(1.86,83.57) = 10.18$, $P < 0.001$, $\eta_p^2 = 0.18$] on RT in the visual search task, but not an interaction effect between these two factors ($P = 0.824$; Figure 2A). Specifically, RTs were faster in LSF [$M(SD) = 540(68)$ ms] than in HSF conditions [548(69) ms], presumably because the more recognizable content in the HSF (*vs* LSF) images interfered more with visual search. In both SF bands, the two threat emotions equivalently ($P = 0.242$) slowed down visual search, in comparison to the neutral condition [fear: 546(69) ms; disgust: 544(68) ms; neutral: 542(69) ms; $P\text{'s} < 0.001$].

Similarly, for response accuracy, a two-way repeated-measures ANOVA revealed a SF effect [$F(1,45) = 13.15$, $P < 0.001$, $\eta_p^2 = 0.23$], a trending emotion effect [$F(1.91,85.77) = 2.62$, $P = 0.082$, $\eta_p^2 = 0.06$], and no interaction between the two factors ($P = 0.622$; Figure 2B). Specifically, higher accuracy was observed in LSF [96.82(2.38) %] than in HSF [96.06(2.92) %] conditions, suggesting, again, more interference caused by the more recognizable HSF images in visual search. The emotion main effect was primarily driven by reduced response accuracy following fear (*vs* neutral) images ($P = 0.017$, $d = -0.37$). Overall, the RT and accuracy results converged to indicate response interference due to threat cues, largely validating our experimental design.

Differential P1 for fear and disgust in HSFs

As illustrated in Figure 3, a two-way ANOVA of Emotion by SF on mean P1 amplitudes revealed a strong SF effect, $F(1,39) = 22.36$, $P < 0.001$, $\eta_p^2 = 0.36$, presumably reflective of physical disparities between HSF and LSF input. Importantly, we uncovered an emotion-by-SF interaction, $F(1.90,73.96) = 8.14$, $P = 0.001$, $\eta_p^2 = 0.17$. Follow-up one-way ANOVAs indicated that in both SF bands, emotion significantly modulated P1 magnitude but in different patterns.

In the HSF condition, the significant emotion effect [$F(1.76,68.72) = 14.64$, $P < 0.001$, $\eta_p^2 = 0.27$] was represented by enlarged P1 to fear images [$M(SD) = 4.80(4.36)$ μV], intermediate to neutral images [3.82(4.74) μV] and dampened to disgust images [3.19(4.89) μV]. Pair-wise comparisons confirmed significant differences between any two emotions [fear *vs* neutral: $t(39) = 3.33$, $P = 0.002$, $d = 0.53$; neutral *vs* disgust: $t(39) = 2.53$, $P = 0.016$, $d = 0.40$; fear *vs* disgust: $t(39) = 4.64$, $P < 0.001$, $d = 0.73$]. Furthermore, point-by-point *t*-tests ascertained that fear-disgust discrimination emerged as early as 109 ms and continued till the end of the epoch—300 ms, while fear and disgust each deviated from the neutral condition starting at 105 and 117 ms, respectively ($P < 0.05$ corrected based on Monte Carlo simulation; Figure 3A).

In the LSF condition, the significant effect of emotion [$F(1.91,74.64) = 4.10$, $P = 0.022$, $\eta_p^2 = 0.10$] had a rather different profile from that in the HSF condition: P1 to LSF disgust was also suppressed [7.31(4.07) μV] in comparison to the LSF neutral condition [8.06(4.14) μV; $t(39) = -3.00$, $P = 0.005$, $d = 0.47$], but P1 to LSF fear [7.63(4.35) μV] did not differ from P1 to the LSF neutral and disgust conditions ($P\text{'s} > 0.148$). Point-by-point *t*-tests further indicated that the LSF disgust waveform deviated from the neutral waveform as early as 82 ms and continued till 133 ms. The fear waveform did not significantly diverge from the other two waveforms in this P1 window.

Using LORETA, we first localized the origin of the P1 potential (collapsed across the three emotions) to the extrastriate cortex for HSF images [cuneus/BA 18, MNI coordinates: peak x, y, $z = -24$, -102, -6] and to the postcentral gyrus in the parietal lobe for LSF images (peak x, y, $z = 18$, -53, 71; Supplementary Figure S1). In support of our ERP extraction and source localization, these source results concurred with the asymmetry of the ventral *vs* dorsal visual stream that HSF *vs* LSF information preferentially activates, respectively (De Valois *et al.*, 1982; Livingstone and Hubel, 1988; Merigan and Maunsell, 1993; Laycock *et al.*, 2007).

Following source validation, we performed voxel-wise *t*-tests in LORETA to isolate neural substrates of the scalp effects in this P1 interval. A cluster was isolated in the left occipital fusiform gyrus in the ventral visual stream [seven voxels; peak: −45, −74, −13; $t(39) = 3.20$, $d = 0.51$; Figure 3C], showing enhanced current density in response to HSF fear than to HSF disgust images. Another cluster was identified in the left precuneus positioned in the dorsal visual stream [three voxels; peak: −24, −88, 36, $t(39) = 3.51$, $d = 0.54$; Figure 3D], exhibiting stronger current density to the LSF neutral than LSF disgust condition. Combined with scalp P1 results, these source analyses confirmed that early visual processing of HSF and LSF threat selectively recruited ventral and dorsal visual pathways, respectively.

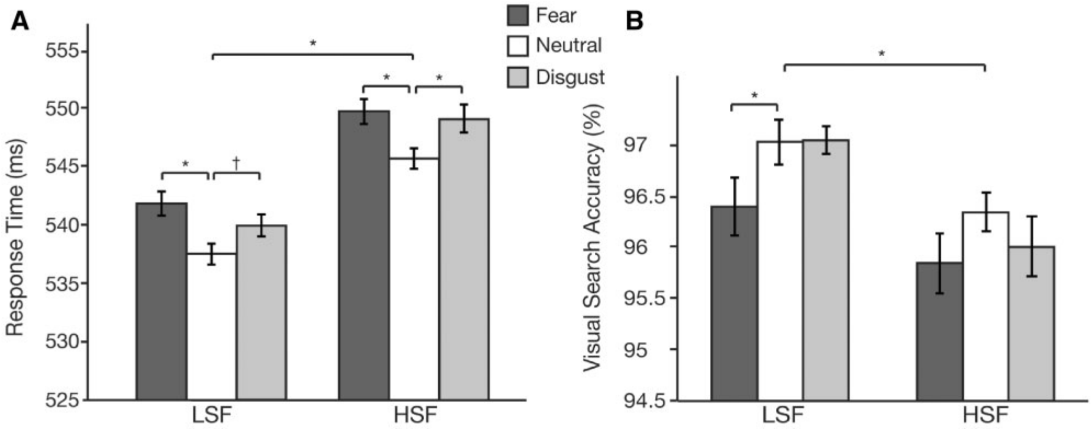

Fig. 2. Behavior results: fear and disgust in both SFs influenced (A) visual search RT and (B) accuracy. *, $P < 0.05$; †, $P < 0.10$; error bars, ± s.e.e. (individually adjusted s.e.m.).

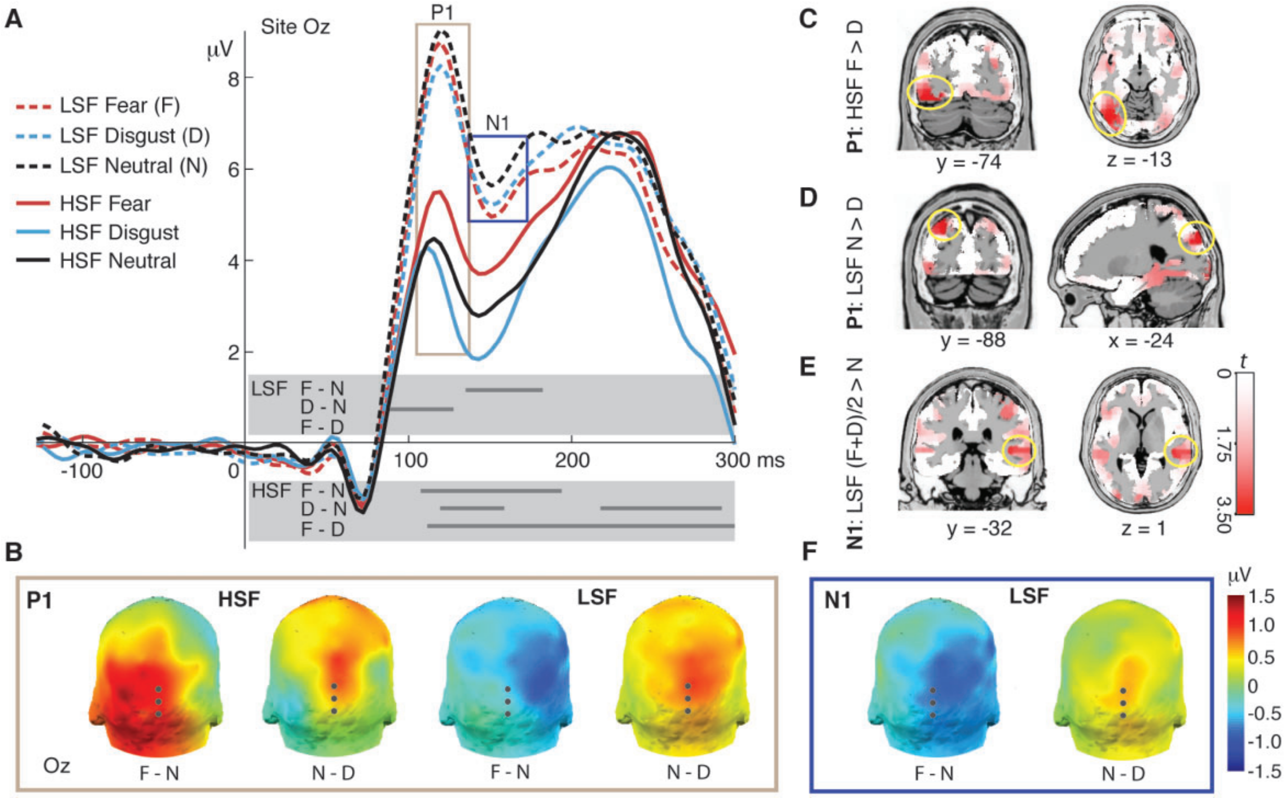

Fig. 3. ERP results: divergent patterns of early visual ERPs to subtypes of threat in HSF and LSF. Grand average ERP waveforms at site Oz show (A) clear P1 and N1 components. Intervals with significant differences between any two conditions are indicated by solid grey lines at the bottom ($P < 0.05$ corrected). For ease of illustration, only the second 100-ms pre-stimulus baseline is shown. Scalp topographies of (B) differential P1 and (F) differential N1 are displayed (gray circled dots represent Oz sensors). LORETA source estimation isolated (C) greater current density for HSF fear over HSF disgust in the left occipital fusiform gyrus during the P1 interval, (D) greater current density for LSF neutral over LSF disgust in the left precuneus during the P1 interval and (E) greater current density for LSF threat (fear and disgust collapsed) than LSF neutral trials in the right middle temporal gyrus during the N1 interval. F, fear; D, disgust; N, neutral.

Critically, the ventral (HSF-sensitive) but not the dorsal (LSF-sensitive) stream was capable of differentiating subordinate-level threat (fear and disgust) during the P1 window.

Overlapping N1 augmentation for fear and disgust in LSFs

A two-way ANOVA on the slightly delayed N1 potential (peaking at 156 ms) yielded both a main effect of SF [$F(1,39) = 14.22$, $P = 0.001$, $\eta_p^2 = 0.27$] and a significant emotion-by-SF interaction effect [$F(1.94,75.47) = 11.98$, $P < 0.001$, $\eta_p^2 = 0.24$; Figure 3A and F]. The main effect of SF was similar to the effect observed in the P1 component with greater mean amplitude in the LSF than HSF.

The emotion-by-SF interaction effect suggested different response profiles during this window in the high and low SFs. As reported earlier, waveforms for fear and disgust in HSFs diverged in opposite directions relative to the neutral condition from 109 ms to the end of epoch; this key pattern was clear in the N1 window [$F(1.79, 69.72) = 16.33$, $P < 0.001$, $\eta_p^2 = 0.30$]. In contrast, for LSF images, we observed a significant effect of emotion on N1 [$F(1.98,77.05) = 3.33$, $P = 0.042$, $\eta_p^2 = 0.08$], driven by enlarged N1 to both LSF fear and disgust relative to the neutral condition [fear *vs* neutral: $t(39) = -2.39$, $P = 0.022$, $d = -0.38$; disgust *vs* neutral, $t(39) = -1.80$, $P = 0.079$, $d = -0.29$; Figure 3A] while the two threat conditions did not differ ($P = 0.442$). Point-by-point *t*-tests further ascertained that LSF fear and disgust waveforms never diverged (at any single time point) throughout the epoch. LORETA source estimation localized the LSF N1 origin (collapsed across the three emotions) to the dorsal visual stream in the postcentral gyrus (peak x, y, $z = 18$, -53, 71; Supplementary Figure S1). A voxel-wise contrast between LSF threat (collapsed across fear and disgust) and LSF neutral conditions specified a cluster in the right middle temporal gyrus, a part of the dorsal visual stream (Ungerleider and Haxby, 1994), which exhibited heightened current density for threat than neutral trials [six voxels; peak: 46, −32, 1; $t(39) = 2.86$, $d = 0.45$; Figure 3E; note: this cluster survived $P < 0.05$ corrected at the voxel level $P < 0.01$].

Control EEG experiment

We then examined ERPs during the P1 and N1 windows in response to phase-scrambled images in the control experiment (Supplementary Figure S2). A two-way ANOVA (Emotion-by-SF) indicated an interaction effect during the P1 interval, $F(1.97,76.74) = 7.15$, $P = 0.002$, $\eta_p^2 = 0.16$. However, the pattern of this effect stood clearly apart from the counterpart in the main experiment. In contrast to the opposite deviation of HSF fear and disgust from the neutral condition in the main experiment, a one-way ANOVA for the HSF condition indicated no main effect of emotion ($P = 0.426$)—the three scrambled emotion conditions had equivalent P1 amplitudes. In contrast to the suppressed P1 to LSF disgust in the main experiment, the ANOVA in the LSF condition revealed a main effect of emotion, $F(1.98,77.10) = 13.45$, $P < 0.001$, $\eta_p^2 = 0.26$, reflecting augmented P1 to scrambled LSF disgust (*vs* scrambled fear and neutral images; P's < 0.002). In the N1 window, a two-way ANOVA revealed a main effect of emotion, $F(1.95,76.14) = 10.11$, $P < 0.001$, $\eta_p^2 = 0.21$, but no emotion-by-SF interaction ($P = 0.248$). Scrambled fear and neutral images evoked greater N1 across LSFs and HSFs than did scrambled disgust images (P's < 0.008). We suspect that these effects could arise from minor physical alterations introduced by the image scramble procedure. Nevertheless, the fact that the pattern of these effects was inconsistent with the pattern of the main effects above largely excluded confounds related to physical disparities across image sets.

Discussion

Using SF filtering of naturalistic images and high-density visual ERPs, we identified both general and specific processing of threat in early visual perception, preferentially tuned to distinctive SF channels and involving segregated visual pathways. Fear and disgust conveyed in HSFs evoked opposite response patterns in the occipital P1 (peaking at 121 ms)—enhanced for fear and suppressed for disgust relative to neutral condition. This divergence was accompanied by heightened activity in the ventral visual (occipital fusiform) cortex for fear *vs* disgust. In contrast, fear and disgust in LSFs elicited convergent response augmentation (*vs* neutral stimuli) in a slightly delayed visual ERP (the N1 peaking at 156 ms), accompanied by overlapping response enhancement for both threats in the middle temporal gyrus (a part of the dorsal visual pathway). These parallel processes align with a recent proposal of multi-path processing of emotion involving amygdala and extra-amygdala pathways (Pessoa and Adolphs, 2010). Furthermore, current findings highlight the coexistence of general, dimensional (threat *vs* neutral) and specific, discrete (fear *vs* disgust) threat characterization in early perception, helping to reconcile the long-standing dimension-*vs*-category debate in emotion research (Ekman, 1994; Russell, 1994; Izard, 1994), supporting hybrid models of emotion (Russell, 2003; Hamann, 2012).

As early visual ERPs are sensitive to physical properties of the stimuli, we carefully equalized the images for size, luminance, contrast and wavelet energy across SF and emotion conditions. In addition, given that SF filtering often introduces visual alterations in images (Vlamings *et al.*, 2009), we took an iterative approach to ensure that the final filtered image sets were comparable in all these basic visual properties. Additional assessment of image complexity and familiarity confirmed that the emotional sets were also equated in these aspects. Furthermore, a control experiment using phase-scrambled versions of the final image sets revealed clearly incompatible results with those in the main analysis, further excluding low-level physical confounds in the P1/N1 effects reported above. Also notably, although a strong asymmetry exists in response to HSF *vs* LSF stimuli in the ventral *vs* dorsal cortical and subcortical visual pathways (De Valois *et al.*, 1982; Livingstone and Hubel, 1988; Merigan and Maunsell, 1993), we acknowledge that this segregation is incomplete and some level of overlap is possible. Nevertheless, this overlap is presumably minor at the moderate contrast and luminance levels applied here (32 and 124/255, respectively). Importantly, our interpretation of the results stands on the relative importance of H/LSF information in these pathways, which is corroborated by our source localization of HSF trials to the ventral visual stream and LSF trials the dorsal visual stream. Moreover, the significant emotion-by-SF interaction effects on P1/N1 potentials further accentuate the relative strengths and dissociable patterns of early visual processing of threat conveyed in low *vs* high SFs. Lastly, as arousal can impact attention and motivation, it may drive the current ERP and behavioral effects, independent of emotion. However, none of the effects were compatible with the systemic decline in rated arousal levels over the three emotions (i.e. fear > disgust > neutral), helping exclude this possible caveat.

It is widely known that threat stimuli evoke enhanced early and late ERPs and hemodynamic responses in multiple brain regions, compared with neutral stimuli (Schupp *et al.*, 2000; Vuilleumier and Pourtois, 2007; Sabatinelli *et al.*, 2011). Specifically, neuroimaging studies have evinced response enhancement to both fear and disgust in the amygdala and OFC (Phillips *et al.*, 1998; Rolls, 2004). In addition, threat analysis in the amygdala and OFC is thought to be preferentially tuned to LSF visual input and largely represent dimensional encoding of affective valence and arousal as opposed to discrete emotions (Barrett and Bar, 2009; Phelps and LeDoux, 2005; Lindquist *et al.*, 2012). In particular, the occipital N1 potential has revealed enhanced visual response to emotional stimuli (Keil *et al.*, 2001, 2002), especially when conveyed in the LSFs (Carretié *et al.*, 2007). Therefore, the convergent augmentation of N1 potentials and dorsal visual activity in response to LSF fear and disgust (*vs* neutral) images confirm this general tenet in the literature, suggesting that early visual processing supports general, dimensional analysis of threat based on reentrant, coarse input from the amygdala/OFC to the visual cortex (Phelps and LeDoux, 2005; Vuilleumier and Pourtois, 2007; Barrett and Bar, 2009; Chikazoe *et al.*, 2014).

In contrast, fear and disgust conveyed in HSFs evoke opposing effects on the P1 component and concomitant occipital fusiform activity. That P1 and ventral cortical activity are heightened for HSF fear and dampened for HSF disgust (relative to neutral trials) maps closely onto our previous findings based on broadband images (Krusemark and Li, 2011, 2013), highlighting a qualitative (*vs* quantitative) dissociation between the two threat subtypes. Importantly, these opposing sensory responses figure nicely with the ecological functions of fear to promote and disgust to suppress sensory acquisition (Susskind *et al.*, 2008) and their distinct effects on perceptual attention and encoding (Krusemark and Li, 2011; Chapman *et al.*, 2013; Van Hooff *et al.*, 2013).

Critically, that four key qualities—specific (subordinate-level) encoding, fast latency, HSF-selectivity, and ventral visual cortical engagement—converge in this threat processing dovetails with standard object categorization in the ventral visual stream that also consummates at 100–150 ms (Van Rullen, 2007; Thorpe, 2009). We thus speculate that with the exception of the few highly preserved, innate objects (e.g. fearful faces) that would elicit enhanced P1 response, especially when presented in LSFs (Pourtois *et al.*, 2005; Vlamings *et al.*, 2009), by activating the superior-colliculus-amygdala pathway (Johnson, 2005), emotion encoding from scenes would involve the visual cortex (Phelps and LeDoux, 2005; Kumar *et al.*, 2012; Krusemark and Li, 2013). The current P1 response to HSF emotional scenes thus raises the possibility that the ventral visual cortex supports specific, categorical threat encoding, in a manner analogous to standard object encoding (Lindquist *et al.*, 2012; Li, 2014). The notion of cortical-based threat processing coincides with accruing evidence of normal rapid threat detection and intact ventral visual cortical response to threat in individuals with extensive or complete amygdala lesion (Tsuchiya *et al.*, 2009; Bach *et al.*, 2011; Piech *et al.*, 2011; Edmiston *et al.*, 2013). Finally, it is worth noting that given opposing effects of threat subtypes on P1 potentials, studies examining these subtypes indiscriminately may fail to demonstrate early visual processing of threat simply due to the cancellation of opposing effects. In fact, from both analytical and theoretical perspectives, there is a growing need to investigate threat at the level of specific subtypes (Weinberg and Hajcak, 2010; Chapman *et al.*, 2013; Wheaton *et al.*, 2013; Van Hooff *et al.*, 2013; Kveraga *et al.*, 2015).

We surmise that HSFs would carry intermediate-level, class-specific sensory features (Ullman *et al.*, 2002), which are 'fear'- and 'disgust-defining' and thus enable discrete categorization of these subtypes even during early stages of perception. Certain sensory rules and regularities have been associated with different emotions. For example, curves are viewed as less threatening and more pleasant than sharp angles (Bar and Neta, 2006, 2007; Larson *et al.*, 2012); HSFs carry diagnostic information for fearful faces; whereas LSFs carry diagnostic information for happy faces and intermediate SFs for disgust faces (Smith and Schyns, 2009). Another possible explanation for this specific threat encoding stems from the associative learning literature, which suggests that plastic changes in the sensory cortex following aversive associative learning would support representation of the newly acquired threat value in the conditioned stimuli (Weinberger, 2007; Li *et al.*, 2008a; Padmala and Pessoa, 2008; Sacco and Sacchetti, 2010; Miskovic and Keil, 2012). Conceivably, by learning to associate a gun with a fear response or a dirty toilet with a disgust response, the ventral visual cortex can develop distinct threat representations associated with corresponding sensory input, thereby supporting specific categorization of fear and disgust even during the initial feedforward sensory sweep (Serre et al. 2007; Weinberger and Bieszczad, 2011; Li, 2014).

Taken together, divergent P1 effects in HSFs and convergent N1 effects in LSFs to fear and disgust implicate the joint participation of ventral visual cortical pathways and dorsal/subcortical (amygdala/OFC-centered) pathways in early threat processing. Accordingly, in naturalistic environments, cortical and subcortical processes act in concert to efficiently capture and analyze threat signals arising in their respectively preferred locations/settings (e.g. fovea or periphery, proximity or distance, light or dark, preferentially recruiting ventral *vs* dorsal/subcortical pathways, respectively), thereby maximizing the biological advantage of the perceiver. Such a system of refined and coarse threat processing in parallel coincides with growing notions in standard object perception, where cortical and subcortical processes operate in concert, and are progressively integrated to drive object perception (Bar, 2003; Bentin *et al.*, 2006; Epstein *et al.*, 2008; Crouzet *et al.*, 2010; Clark, 2013). Therefore, it is possible that threat perception entails a specifically tuned cortical pathway for precise threat categorization to inform discrete emotion responses, and a broadly tuned amygdala/OFC pathway for sensitive threat detection to prompt general defense response (Li, 2014). Last, we surmise that as the two pathways interact intimately, output of the detailed sensory cortical encoding of threat signals is progressively integrated with the product of amygdala/OFC processing, activating the defense system in a dimensional manner (Krusemark and Li, 2013). Consequently, HSF and LSF threat could trigger overlapping defense responses and behavior, such as the convergent visual search interference by fear and disgust in both SF bands demonstrated here.

In sum, current findings lend support to the notion of parallel general and specific processing of threat involving different neural pathways, even at a very early stage (Pessoa and Adolphs, 2010). Such integrative, parallel processing would afford critical ecological advantages, facilitating perception and evaluation of danger in the environment. Last, parallel processing of general and specific threat can help to reconcile long-standing debates in emotion conceptualization (Cacioppo and Berntson, 1994; Ekman, 1994; Izard, 1994; Russell, 1994), in support of emerging hybrid models (Russell, 2003; Hamann, 2012) incorporating both categorical and dimensional aspects of emotion.

Acknowledgements

We thank Lyn Abramson, Lucas Novak, Bas Rokers for helpful comments.

Funding

This research was supported by the National Institute of Mental Health (R01MH093413 to W.L.).

Supplementary data

Supplementary data are available at *SCAN* online.

Conflict of interest. None declared.

References

Anderson, A.K., Christoff, K., Panitz, D., De Rosa, E., Gabrieli, J.D.E. (2003). Neural correlates of the automatic processing of threat facial signals. *The Journal of Neuroscience*, **23**(13), 5627–33.

Alorda, C., Serrano-Pedraza, I., Campos-Bueno, J.J., Sierra-Vázquez, V., Montoya, P. (2007). Low spatial frequency filtering modulates early brain processing of affective complex pictures. *Neuropsychologia*, **45**(14), 3223–33.

Bach, D.R., Talmi, D., Hurlemann, R., Patin, A., Dolan, R. (2011). Automatic relevance detection in the absence of a functional amygdala. *Neuropsychologia*, **49**(5), 1302–5.

Bar, M. (2003). A cortical mechanism for triggering top-down facilitation in visual object recognition. *Journal of Cognitive Neuroscience*, **15**, 600–9.

Bar, M., Neta, M. (2006). Humans prefer curved visual objects. *Psychological Science*, **17**(8), 645–8.

Bar, M., Neta, M. (2007). Visual elements of subjective preference modulate amygdala activation. *Neuropsychologia*, **45**(10), 2191–200.

Barrett, L.F., Bar, M. (2009). See it with feeling: affective predictions during object perception. *Philosophical Transactions of the Royal Society of London. Series B, Biological Sciences*, **364**(1521), 1325–34.

Bentin, S., Golland, Y., Flevaris, A., Robertson, L.C., Moscovitch, M. (2006). Processing the trees and the forest during initial stages of face perception: electrophysiological evidence. *Journal of Cognitive Neuroscience,* **18**(8), 1406–21.

Cacioppo, J., Berntson, G. (1994). Relationship between attitudes and evaluative space: a critical review, with emphasis on the separability of positive and negative substrates. *Psychological Bulletin*, **115**(3), 401–23.

Carretié, L., Hinojosa, J.A., Martín-Loeches, M., Mercado, F., Tapia, M. (2004). Automatic attention to emotional stimuli: neural correlates. *Human Brain Mapping*, **22**(4), 290–99.

Carretié, L., Hinojosa, J.A., López-Martín, S., Tapia, M. (2007). An electrophysiological study on the interaction between emotional content and spatial frequency of visual stimuli. *Neuropsychologia*, **45**(6), 1187–95.

Chapman, H. A., Johannes, K., Poppenk, J.L., Moscovitch, M., Anderson, A. K. (2013). Evidence for the differential salience of disgust and fear in episodic memory. *Journal of Experimental Psychology: General*, **142**(4), 1100–12.

Chen, C.-C., Kao, K.-L.C., Tyler, C.W. (2007). Face configuration processing in the human brain: the role of symmetry. *Cerebral Cortex*, **17**(6), 1423–32.

Chikazoe, J., Lee, D.H., Kriegeskorte, N., Anderson, A.K. (2014). Population coding of affect across stimuli, modalities and individuals. *Nature Neuroscience,* **17**, 1114–22.

Clark, A. (2013). Whatever next? Predictive brains, situated agents, and the future of cognitive science. *Behavioral and Brain Sciences*, **36**(3), 181–204.

Crouzet, S., Kirchner, H., Thorpe, S. (2010). Fast saccades toward faces: face detection in just 100 ms. *Journal of Vision*, **10**, 1–17.

De Cesarei, A., Mastria, S., Codispoti, M. (2013). Early spatial frequency processing of natural images: an ERP study. *PLoS One,* **8**(5), e65103.

De Valois, R., Albrecht, D., Thorell, L. (1982). Spatial frequency selectivity of cells in macaque visual cortex. *Vision Research,* **22**(5), 545–59.

Delplanque, S., N'diaye, K., Scherer, K., Grandjean, D. (2007). Spatial frequencies or emotional effects? A systematic measure of spatial frequencies for IAPS pictures by a discrete wavelet analysis. *Journal of Neuroscience Methods*, **165**(1), 144–50.

Edmiston, E.K., McHugo, M., Dukic, M.S., *et al.* (2013). Enhanced visual cortical activation for emotional stimuli is preserved in patients with unilateral amygdala resection. *The Journal of Neuroscience*, **33**(27), 11023–31.

Eimer, M., Holmes, A. (2007). Event-related brain potential correlates of emotional face processing. *Neuropsychologia*, **45**(1), 15–31.

Ekman, P. (1992). An argument for basic emotions. *Cognition and Emotion*, **6**, 169–200.

Ekman, P. (1994). Strong evidence for universals in facial expressions: a reply to Russell's mistaken critique. *Psychological Bulletin*, **115**(2), 268–87.

Epstein, R.A. (2008). Parahippocampal and retrosplenial contributions to human spatial navigation. *Trends in Cognitive Sciences*, **12**(10), 388–96.

Flaisch, T., Schupp, H. T. (2013). Tracing the time course of emotion perception: the impact of stimulus physics and semantics on gesture processing. *Social Cognitive and Affective Neuroscience*, **8**(7), 820–7.

Flevaris, A., Bentin, S., Robertson, L. (2010). Local or Global? Attentional selection of spatial frequencies binds shapes to hierarchical levels. *Psychological Science*, **21**(3), 424–31.

Forscher, E.C., Li, W. (2012). Hemispheric asymmetry and visuo-olfactory integration in perceiving subthreshold (micro) fearful expressions. *The Journal of Neuroscience*, **32**(6), 2159–65.

Gray, J.A. (1987). *The Psychology of Fear and Stress. American Journal of Psychiatry*. New York, NY: Cambridge University Press.

Hamann, S. (2012). Mapping discrete and dimensional emotions onto the brain: controversies and consensus. *Trends in Cognitive Sciences*, **16**(9), 458–66.

Han, S., Yund, E.W., Woods, D.L. (2003). An ERP study of the global precedence effect: the role of spatial frequency. *Clinical Neurophysiology*, **114**(10), 1850–65.

Hot, P., Saito, Y., Mandai, O., Kobayashi, T., Sequeira, H. (2006). An ERP investigation of emotional processing in European and Japanese individuals. *Brain Research*, **1122**(1), 171–8.

Hillyard, S.A., Anllo-Vento, L. (1998). Event-related brain potentials in the study of visual selective attention. *Proceedings of the National Academy of Sciences*, **95**(3), 781–7.

Hughes, H.C., Fendrich, R., Reuter-Lorenz, P.A. (1990). Global versus local processing in the absence of low spatial frequencies. *Journal of Cognitive Neuroscience*, **2**(3), 272–282.

Izard, C. (1994). Innate and universal facial expressions: evidence from developmental and cross-cultural research. *Psychological Bulletin*, **115**(2), 288–99.

Johnson, M.H. (2005). Subcortical face processing. *Nature Reviews Neuroscience*, **6**(10), 766–74.

Kauffmann, L., Ramanoël, S., Guyader, N., Chauvin, A., Peyrin, C. (2015). Spatial frequency processing in scene-selective cortical regions. *NeuroImage*, **112**, 86–95.

Kawasaki, H., Tsuchiya, N., Kovach, C.K., Nourski, K.V., Oya, H., Howard, M.A., Adolphs, R. (2012). Processing of facial emotion in the human fusiform gyrus. *Journal of Cognitive Neuroscience*, **24**(6), 1358–1370.

Keil, A., Bradley, M.M., Hauk, O., Rockstroh, B., Elbert, T., Lang, P.J. (2002). Large-scale neural correlates of affective picture processing. *Psychophysiology*, **39**(5), 641–9.

Keil, A., Müller, M.M., Gruber, T., Wienbruch, C., Stolarova, M., Elbert, T. (2001). Effects of emotional arousal in the cerebral hemispheres: a study of oscillatory brain activity and event-related potentials. *Clinical Neurophysiology*, **112**(11), 2057–68.

Krusemark, E.A., Novak, L.R., Gitelman, D.R., Li, W. (2013). When the sense of smell meets emotion: anxiety-state-dependent olfactory processing and neural circuitry adaptation. *The Journal of Neuroscience*, **33**(39), 15324–32.

Krusemark, E.A., Li, W. (2011). Do all threats work the same way? Divergent effects of fear and disgust on sensory perception and attention. *The Journal of Neuroscience*, **31**(9), 3429–34.

Krusemark, E.A., Li, W. (2013). From early sensory specialization to later perceptual generalization: dynamic temporal progression in perceiving individual threats. *The Journal of Neuroscience*, **33**(2), 587–94.

Kumar, S., von Kriegstein, K., Friston, K., Griffiths, T. D. (2012). Features versus feelings: dissociable representations of the acoustic features and valence of aversive sounds. *The Journal of Neuroscience*, **32**(41), 14184–92.

Kveraga, K., Boshyan, J., Bar, M. (2007). Magnocellular projections as the trigger of top-down facilitation in recognition. *The Journal of Neuroscience*, **27**(48), 13232–40.

Kveraga, K., Boshyan, J., Adams, R.B., *et al.* (2015). If it bleeds, it leads: separating threat from mere negativity. *Social Cognitive and Affective Neuroscience,* **10**(1), 28–35.

Lang, P., Bradley, M., Cuthbert, B. (2008). International Affective Picture System (IAPS): affective ratings of pictures and instruction manual. *Technical report A*-8. Gainesville, FL: University of FLorida.

Larson, C., Aronoff, J., Steuer, E. (2012). Simple geometric shapes are implicitly associated with affective value. *Motivation and Emotion,* **36**(3), 404–13.

Laycock, R., Crewther, S. G., Crewther, D. P. (2007). A role for the "magnocellular advantage" in visual impairments in neurodevelopmental and psychiatric disorders. *Neuroscience and Biobehavioral Reviews*, **31**(3), 363–76.

Li, W. (2014). Learning to smell danger: acquired associative representation of threat in the olfactory cortex. *Frontiers in Behavioral Neuroscience*, **8**(April), 1–8.

Li, W., Howard, J.D., Parrish, T.B., Gottfried, J.A. (2008a). Aversive learning enhances perceptual and cortical discrimination of indiscriminable odor cues. *Science*, **319**(5871), 1842–1845.

Li, W., Zinbarg, R.E., Boehm, S.G., Paller, K.A. (2008b). Neural and behavioral evidence for affective priming from unconsciously perceived emotional facial expressions and the influence of trait anxiety. *Journal of Cognitive Neuroscience*, **20**(1), 2095–107.

Lindquist, K.A., Wager, T.D., Kober, H., Bliss-Moreau, E., Barrett, L.F. (2012). The brain basis of emotion: a meta-analytic review. *The Behavioral and Brain Sciences*, **35**(3), 121–43.

Liu, Y., Zhang, D., Luo, Y. (2015). How disgust facilitates avoidance: an ERP study on attention modulation by threats. *Social Cognitive and Affective Neuroscience*, **10**(4), 598–604.

Livingstone, M., Hubel, D. (1988). Segregation of form, color, movement, and depth: anatomy, physiology, and perception. *Science*, **240**(4853), 740–9.

Loftus, G.R., Harley, E.M. (2005). Why is it easier to identify someone close than far away? *Psychonomic Bulletin Review*, **12**(1), 43–65.

Mangun, G.R., Hillyard, S.A., Luck, S.J. (1993). Electrocortical substrates of visual selective attention. In Meyer, D.E., Kornblum, S., editors. *Attention and Performance XIV: Synergies in Experimental Psychology, Artificial Intelligence and Cognitive Neuroscience*, pp. 219–43. Cambridge, MA: MIT Press.

Marin, M.M., Leder, H. (2013). Examining complexity across domains: relating subjective and objective measures of affective environmental scenes, paintings and music. *PloS One*, **8**(8), e72412.

McNally, R.J. (2002). Disgust has arrived. *Journal of Anxiety Disorders*, **16**(5), 561–6.

Merigan, W.H., Maunsell, J.H. (1993). How parallel are the primate visual pathways? *Annual Review of Neuroscience*, **16**(1), 369–402.

Miskovic, V., Keil, A. (2012). Acquired fears reflected in cortical sensory processing: a review of electrophysiological studies of human classical conditioning. *Psychophysiology*, **49**(9), 1230–41.

Neuberg, S.L., Kenrick, D.T., Schaller, M. (2011). Human threat management systems: self-protection and disease avoidance. *Neuroscience and Biobehavioral Reviews*, **35**(4), 1042–51.

Oaten, M., Stevenson, R.J., Case, T.I. (2009). Disgust as a disease-avoidance mechanism. *Psychological Bulletin*, **135**(2), 303–21.

Olofsson, J.K., Nordin, S., Sequeira, H., Polich, J. (2008). Affective picture processing: an integrative review of ERP findings. *Biological Psychology*, **77**(3), 247–65.

Padmala, S., Pessoa, L. (2008). Affective learning enhances visual detection and responses in primary visual cortex. *The Journal of Neuroscience*, **28**(24), 6202–10.

Pascual-Marqui, R.D., Esslen, M., Kochi, K., Lehmann, D. (2002). Functional imaging with low-resolution brain electromagnetic tomography (LORETA): a review. *Methods and Findings in Experimental and Clinical Pharmacology*, **24**(Suppl C), 91–5.

Pessoa, L., Adolphs, R. (2010). Emotion processing and the amygdala: From a "low road" to "many roads" of evaluating biological significance. *Nature Reviews Neuroscience*, **11**(11), 773–83.

Phelps, E.A., LeDoux, J.E. (2005). Contributions of the amygdala to emotion processing: from animal models to human behavior. *Neuron*, **48**(2), 175–87.

Phillips, M.L., Young, A.W., Scott, S.K., *et al.* (1998). Neural responses to facial and vocal expressions of fear and disgust. *Proceedings of the Royal Society B: Biological Sciences*, **265**(1408), 1809–17.

Piech, R.M., McHugo, M., Smith, S.D., *et al.* (2011). Attentional capture by emotional stimuli is preserved in patients with amygdala lesions. *Neuropsychologia*, **49**(12), 3314–9.

Pizzagalli, D.A., Greischar, L.L., Davidson, R.J. (2003). Spatiotemporal dynamics of brain mechanisms in aversive classical conditioning: high-density event-related potential and brain electrical tomography analyses. *Neuropsychologia*, **41**(2), 184–94.

Pourtois, G., Dan, E.S., Grandjean, D., Sander, D., Vuilleumier, P. (2005). Enhanced extrastriate visual response to bandpass spatial frequency filtered fearful faces: time course and topographic evoked-potentials mapping. *Human Brain Mapping*, **26**(1), 65–79.

Robertson, L.C. (1996). Attentional persistence for features of hierarchical patterns. *Journal of Experimental Psychology: General*, **125**(3), 227–49.

Rolls, E.T. (2004). The functions of the orbitofrontal cortex. *Brain and Cognition*, **55**(1), 11–29.

Rosenholtz, R., Li, Y., Nakano, L. (2007). Measuring visual clutter. *Journal of Vision*, **7**(2), 17.

Rossignol, M., Campanella, S., Maurage, P., Heeren, A., Falbo, L., Philippot, P. (2012). Enhanced perceptual responses during visual processing of facial stimuli in young socially anxious individuals. *Neuroscience Letters*, **526**(1), 68–73.

Rozin, P., Fallon, A. (1987). A perspective on disgust. *Psychological Review*, **94**, 23–41.

Russell, J.A. (1980). A circumplex model of affect. *Journal of Personality and Social Psychology*, **39**(6), 1161–78.

Russell, J.A. (1994). Is there universal recognition of emotion from facial expressions? A review of the cross-cultural studies. *Psychological Bulletin*, **115**(1), 102–41.

Russell, J.A. (2003). Core affect and the psychological construction of emotion. *Psychological Review*, **110**(1), 145–72.

Sabatinelli, D., Fortune, E.E., Li, Q., Siddiqui, A., Krafft, C., Oliver, W.T., Beck, S., Jeffries, J. (2011). Emotional perception: meta-analyses of face and natural scene processing. *NeuroImage*, **54**(3), 2524–33.

Sacco, T., Sacchetti, B. (2010). Role of secondary sensory cortices in emotional memory storage and retrieval in rats. *Science*, **329**(5992), 649–56.

Schyns, P., Oliva, A. (1994). From blobs to boundary edges: evidence for time- and spatial-scale-dependent scene recognition. *Psychological Science*, **5**(4), 195–200.

Schupp, H.T., Cuthbert, B.N., Bradley, M.M., Cacioppo, J.T., Ito, T., Lang, P.J. (2000). Affective picture processing: the late positive potential is modulated by motivational relevance. *Psychophysiology,* **37**, 257–61.

Serre, T., Oliva, A., Poggio, T. (2007). A feedforward architecture accounts for rapid categorization. *Proceedings of the National Academy of Sciences of the United States of America*, **104**(15), 6424–9.

Shulman, G., Wilson, J. (1987). Spatial frequency and selective attention to global and local information. *Perception*, **16**, 89–101.

Smith, F. W., Schyns, P. G. (2009). Smile through your fear and sadness: transmitting and identifying facial expression signals over a range of viewing distances. *Psychological Science*, **20**(10), 1202–8.

Smith, N.K., Cacioppo, J.T., Larsen, J.T., Chartrand, T.L. (2003). May I have your attention, please: electrocortical responses to positive and negative stimuli. *Neuropsychologia*, **41**(2), 171–83.

Steinberg, C., Bröckelmann, A., Rehbein, M., Dobel, C., Junghöfer, M. (2013). Rapid and highly resolving associative affective learning: convergent electro-and magnetoencephalographic evidence from vision and audition. *Biological Psychology*, **92**(3), 526–40.

Stolarova, M., Keil, A., Moratti, S. (2006). Modulation of the C1 visual event-related component by conditioned stimuli: evidence for sensory plasticity in early affective perception. *Cerebral Cortex*, **16**(6), 876–87.

Susskind, J.M., Lee, D.H., Cusi, A., Feiman, R., Grabski, W., Anderson, A.K. (2008). Expressing fear enhances sensory acquisition. *Nature Neuroscience*, **11**(7), 843–50.

Thatcher, R.W., North, D., Biver, C. (2005). Evaluation and validity of a LORETA normative EEG database. *Clinical EEG and Neuroscience*, **36**(2), 116–22.

Thorpe, S.J. (2009). The speed of categorization in the human visual system. *Neuron*, **62**(2), 168–70.

Tsuchiya, N., Moradi, F., Felsen, C., Yamazaki, M., Adolphs, R. (2009). Intact rapid detection of fearful faces in the absence of the amygdala. *Nature Neuroscience*, **12**(10), 1224–5.

Ullman, S., Vidal-Naquet, M., Sali, E. (2002). Visual features of intermediate complexity and their use in classification. *Nature Neuroscience*, **5**(7), 682–7.

Ungerleider, L.G., Haxby, J.V. (1994). “What” and “where” in the human brain. *Current Opinion in Neurobiology*, **4**(2), 157–65.

Van Hooff, J.C., Devue, C., Vieweg, P.E., Theeuwes, J. (2013). Disgust-and not fear-evoking images hold our attention. *Acta Psychologica*, **143**(1), 1–6.

Van Rullen, R. (2007). The power of the feed-forward sweep. *Advances in Cognitive Psychology*, **3**(1–2), 167–76.

Vlamings, P.H.J.M., Goffaux, V., Kemner, C. (2009). Is the early modulation of brain activity by fearful facial expressions primarily mediated by coarse low spatial frequency information? *Journal of Vision*, **9**(5), 1–13.

Vogel, E.K., Luck, S.J. (2000). The visual N1 component as an index of a discrimination process. *Psychophysiology*, **37**(2), 190–203.

Vuilleumier, P., Armony, J.L., Driver, J., Dolan, R.J. (2003). Distinct spatial frequency sensitivities for processing faces and emotional expressions. *Nature Neuroscience*, **6**(6), 624–31.

Vuilleumier, P., Pourtois, G. (2007). Distributed and interactive brain mechanisms during emotion face perception: evidence from functional neuroimaging. *Neuropsychologia*, **45**(1), 174–94.

Weinberg, A., Hajcak, G. (2010). Beyond good and evil: the time-course of neural activity elicited by specific picture content. *Emotion,* **10**(6), 767–82.

Weinberg, A., Hajcak, G. (2011). Electrocortical evidence for vigilance-avoidance in Generalized Anxiety Disorder. *Psychophysiology*, **48**(6), 842–51.

Weinberger, N.M. (2007). Associative representational plasticity in the auditory cortex: a synthesis of two disciplines. *Learning and Memory*, **14**, 1–16.

Weinberger, N.M., Bieszczad, K.M. (2011). Introduction: from traditional fixed cortical sensationism to contemporary plasticity of primary sensory cortical representations. In: Gottfried, J.A., editor, pp. 3–13. *Neurobiology of Sensation and Reward*. BocaRaton, FL: CRCPress.

Wheaton, M.G., Holman, A., Rabinak, C.A., Macnamara, A., Proudfit, G.H., Phan, K.L. (2013). Danger and disease: electrocortical responses to threat- and disgust-eliciting images. *International Journal of Psychophysiology*, **90**(2), 235–9.

Willenbockel, V., Sadr, J., Fiset, D., Horne, G.O., Gosselin, F., Tanaka, J. W. (2010). Controlling low-level image properties: the SHINE toolbox. *Behavior Research Methods*, **42**(3), 671–84.

Williams, L.M., Kemp, A.H., Felmingham, K., Liddell, B.J., Palmer, D.M., Bryant, R.A. (2007). Neural biases to covert and overt signals of fear: dissociation by trait anxiety and depression. *Journal of Cognitive Neuroscience*, **19**(10), 1595–608.

Winston, J.S., Vuilleumier, P., Dolan, R.J. (2003). Effects of low-spatial frequency components of fearful faces on fusiform cortex activity. *Current Biology*, **13**(20), 1824–9.

Yoshida, T., Yoshino, A. (2007). Comparison of hemispheric asymmetry in global and local information processing and interference in divided and selective attention using spatial frequency filters. *Experimental Brain Research*, **181**(3), 519–29.